

Review

Polyelectrolyte Multilayers: Towards Single Cell Studies

Dmitry Volodkin ^{1,*}, Regine von Klitzing ² and Helmuth Moehwald ³

¹ Fraunhofer Institute for Biomedical Engineering, Am Mühlenberg 13, Potsdam-Golm 14476, Germany

² Stranski-Laboratorium für Physikalische und Theoretische Chemie, Institut für Chemie, Technische Universität Berlin, Strasse des 17. Juni 124, Berlin 10623, Germany; E-Mail: klitzing@mailbox.tu-berlin.de

³ Department of Interfaces, Max-Planck Institute for Colloids and Interfaces, Am Mühlenberg 1, Potsdam-Golm 14476, Germany; E-Mail: helmuth.moehwald@mpikg.mpg.de

* Author to whom correspondence should be addressed;

E-Mail: dmitry.volodkin@ibmt.fraunhofer.de; Tel.: +49-331-58187-327; Fax: +49-331-58187-399.

Received: 3 March 2014; in revised form: 30 April 2014 / Accepted: 3 May 2014 /

Published: 20 May 2014

Abstract: Single cell analysis (SCA) is nowadays recognized as one of the key tools for diagnostics and fundamental cell biology studies. The Layer-by-layer (LbL) polyelectrolyte assembly is a rather new but powerful technique to produce multilayers. It allows to model the extracellular matrix in terms of its chemical and physical properties. Utilization of the multilayers for SCA may open new avenues in SCA because of the triple role of the multilayer film: (i) high capacity for various biomolecules; (ii) natural mimics of signal molecule diffusion to a cell and (iii) cell patterning opportunities. Besides, light-triggered release from multilayer films offers a way to deliver biomolecules with high spatio-temporal resolution. Here we review recent works showing strong potential to use multilayers for SCA and address accordingly the following issues: biomolecule loading, cell patterning, and light-triggered release.

Keywords: layer-by-layer; thin films; capsule; release; cell patterning; multilayer

1. Introduction

Traditionally, bioanalytical studies have been performed for a rather large group of cells (from thousands to millions) yielding an average value of a certain cellular response or of a concentration of the cell-expressed analytes. Single cell analysis (SCA) focuses on the level of a single cell. Over the

last decade SCA has attracted special attention because it provides an option to analyze the content and behavior of individual cells [1]. The SCA is promising from both applied and fundamental aspects. From an applied point of view a clinical analysis of a low number of cells is indispensable for rare cells such as circulating tumor cells, cell co-cultures, embryonic bodies, *etc.* At the same time, the fundamental interest arises from the heterogeneity of biological cells in their composition and also their functions [2,3]. Thus, thanks to SCA new effective diagnostics approaches and new insights in cell biology, genomics, proteomics and other biologically relevant fields have been already reported or are expected in the near future. A number of modern techniques have been developed for SCA including fluorescence methods, capillary electrophoresis, microfluidics, mass spectroscopy, *etc.* [4,5]. Mostly, these techniques are advantageous due to analysis of small volumes and due to increased sensitivity of analyte detection (e.g., by microfluidics).

The LbL polymer deposition [6,7] is nowadays well recognized as a powerful technique to engineer surfaces and free-standing films due to the capability of easily tuning the physical and chemical film properties basically by a number of deposited layers or deposition conditions [8–11]. Bioapplications of the LbL films have attracted special attention because of a fine control over composition and mechanical properties of the films. Bioapplications of stimuli-responsive films and capsules have been extensively reviewed focusing on cellular response and film biofunctionalization [12–19]. The LbL films play the role of reservoirs providing a living organism with the required bioactive molecules such as growth factors, drugs, DNA, peptides or other soluble and insoluble signaling factors [15,20–24]. The reservoir capacity may be extremely high due to the large number of free polymer groups and the mobility of polymer molecules in the film [15,25]. The LbL technique can be considered as one of the very promising approaches to engineer the artificial extracellular matrix (ECM) [26,27]. The latter is an ultimate goal for modeling a real cellular microenvironment that allows the direct comparison of *in vitro* and *in vivo* cellular behavior [28].

Besides, LbL films are effective coatings to govern cellular adhesion. The soft nature of highly hydrated LbL films such as model films from hyaluronic acid (HA) and polylysine (PLL) [29,30] results typically in cellular repellent properties [31–33]. However, the improvement of the mechanical properties of soft LbL films leads to a better cellular adhesion. This may be achieved by different ways. Chemical crosslinking has been extensively studied [34,35]. Physical crosslinking of the upper film part allows maintaining the chemical composition of the main part of the film intact [36]. The whole film can be also made stiffer if one uses stiff nanoparticles to produce multilayers [37]. Another option is to introduce additional polymer “layers” making the film stiffer due to formation of less hydrated capping layers (usually from highly charged synthetic polymers) on the film top [33,38]. Patterning of the LbL films by a combination of microfluidics and stamping technique without any chemical or physical influence on the film properties has been recently demonstrated [39]. This might be a perfect option to establish cellular patterns in unmodified (native) LbL films, as has been shown recently.

The LbL films may not only host biomolecules but also enable their release on demand. Some extensive reviews can be found on biological applications of stimuli-sensitive multilayers changing their structure as a function of the following stimuli: pH, ionic strength, electrical potential, biologically active compounds, temperature, deformation, *etc.* [9,10,12–14,40]. At the same time, remote stimuli such as light, ultrasound, magnetic field have not been widely investigated for biologically relevant

LbL films, for instance films made of biopolymers. Among the externally applied stimuli near infra-red (IR)-light (650–1000 nm) seems to be the most promising one because of its non-invasive character, easy modulation of light power and wavelength, and focusing light with micrometer precision. Besides, IR-light can penetrate through soft tissues to the depth of up to several cm due to low absorption by tissue constituents [41,42]. With respect to the film release properties, one has to emphasize the main advantage of the LbL films made of ECM components if compared to established approaches for delivery of signal molecules such as microfluidics [43]. The advantage is that the signaling molecules diffusing through such films to a cell (seeded on the film top) are delivered in a natural way-by diffusion through the artificial ECM network created by the film. Thus, more reliable results with respect to natural cellular behavior could be obtained.

The use of LbL films for SCA may, according to our opinion, bring new opportunities into the field of SCA, because the films may not only provide enough signal molecules to a cell by a natural way but also allow many options for the positioning and the selective growth of cells. However, to the best of our knowledge the polyelectrolyte LbL films have until now not been widely used for SCA. This area is just developing, but relatively high number of recent works highlighted in this review point at the high potential of the LbL films for SCA. This motivates us to review recent achievements towards this new field. Here we focus on the main features of LbL films necessary to employ them for SCA: reservoir properties for bioactive molecules, cell patterning approaches, and externally stimulated (light-triggered) biomolecule release. Finally we show future perspectives of the employment of LbL assembled films for SCA.

2. LbL Films as Carriers for Bioactive Substances

2.1. Control of the Structure and Dynamics of LbL Films

The ability to uptake and release drugs (e.g., proteins and nanoparticles) depends on the porosity and mesh size within the LbL films as well as physicochemical properties of the film such as hydrophilic-hydrophobic balance, charge balance, *etc.* It has also a strong impact on the protein folding of embedded proteins. If the mesh size does not fit to the enzyme size the enzyme can be converted into its inactive form. The LbL films can be considered as a network that is physically cross-linked by polyanion-polycation complexation sites. The mesh sizes are mainly determined by the number density of complexation sites. In order to control the uptake and release of drugs or other additives, these sites have to be tailored and triggered by external stimuli like pH, ionic strength or temperature. By this, the cross-link points can be opened and closed in a controlled way. The big advantage of LbL films in comparison to inorganic porous materials is that the pores (or meshes) are flexible with certain dynamics. The flexibility can be varied as well. LbL films with a high density of complexation sites are more rigid and show a lower ability to respond to outer stimuli than LbL films with a lower density. On the other hand the LbL films become unstable if the cross-linker density is too low. In order to use them for SCA the LbL films have to be balanced between the two counteracting properties of long-term stability and sensitivity to outer stimuli.

To summarize: in order to get a versatile polymer matrix for SCA, the density and strength of the complexation sites have to be controlled. There are many parameters to tune the structure and

dynamics of LbL films. Some of them are presented in the following. A more detailed description is given in the following reviews [6,11,44–46].

In general, the number density of complexation sites is high if both polyanion and polycation have a high charge density, determined by synthesis and/or pH of the environment. The complexation between polyanions and polycations is entropically driven due to a strong gain in entropy during counterion release. The charge density plays a crucial role in the film growth regime, which is defined by the strength of interpolymer interactions. *Intrinsic* compensation takes place if the polyelectrolyte charges are compensated by the charge of the oppositely charged polyelectrolyte. Poly(styrene sulphonate)/poly(allylamine hydrochloride) (PSS/PAH) is an example for a rigid and immobile system with a linear growth [47]. Both PAH and PSS have a high charge density, the polymers do not diffuse in the film because of strong interaction. On the other hand, if at least one of the polymers has a low charge density the matrix is rather mobile. In this case, *extrinsic* charge compensation takes place, *i.e.*, charge is mostly compensated by counterions. Due to lower number of contacts between polymer, the strength of interpolymer interaction is lower than in case of *intrinsic* compensation. HA/PLL is the most popular example for this type of systems with an exponential growth, *i.e.*, the thickness increases exponentially with the number of deposition steps [48]. In case of exponential growth at least one of the polyelectrolytes is able to diffuse into the polyelectrolyte multilayers (PEM) which is demonstrated below in Confocal Laser Scanning Microscopy (CLSM) studies. Recently, the diffusion of one polyelectrolyte species was proved by identifying excess polyelectrolyte charges within the LbL film [49].

The polyanion/polycation interactions compete with interactions of the polyelectrolytes and their counterions, especially if an excess is offered by addition of high salt concentration. This might destroy some complexes, and *extrinsic* charge compensation of the polyelectrolyte could take place. This is even more pronounced in the presence of counterions with a low charge density like Cs^+ or Br^- . Due to their small hydration shell they easily interact with the oppositely charged groups of polyelectrolytes [50]. The consequence is a lower density of complexation sites. This in turn leads to thicker films with a more mobile polymer matrix [47] related to an exponential growth with endothermic formation of complexes [51]. In case of pronounced *extrinsic* charge compensation the LbL films are denser with fewer voids in the dry state due to stronger screening of the polyelectrolyte charges [52]. This gives a higher flexibility of the polymer chains and an easier adjustment of the chains to the environment. In contrast, these LbL films swell more strongly in water than the ones built up in presence of small ions. Due to the lower density of complexation sites the mesh sizes are larger and can take up more water [52]. The same phenomenon was observed for increasing salt concentration during film formation.

Further competing interactions are the solubility of the polyanion-polycation complexes *vs.* the interactions between the complexes with the surface. The different interactions offer a wide field to adjust the polyelectrolyte multilayer with respect to the needed purpose. LbL films built-up in presence of larger ions are less stable. In the case of a strong decrease in the number of complexation sites due to strong polyion-interactions and/or high ionic strength the formation of LbL films might even become impossible [53].

Besides loading LbL films with additives after preparation, they can also be directly incorporated during LbL film formation. Biomolecules like proteins, peptides and DNA replace one of the polyelectrolytes, and they can be combined with an oppositely charged polyelectrolyte. A similar

approach is possible with charged nanoparticles or objects like vesicles, liposomes, *etc.* as will be shown below. Especially for directed charge transfer a polarity gradient is necessary which can be formed by combination of different polyelectrolytes [54].

2.2. Loading of Biomolecules

2.2.1. Loading with Small Molecules

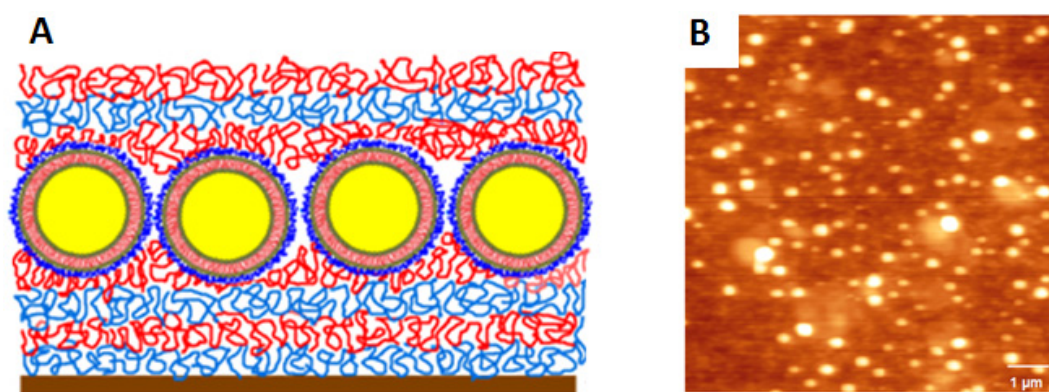
Firstly, we will focus on the loading with small molecules, either dyes as model drugs or pharmaceuticals. Pharmaceuticals can be directly loaded by the post-loading approach (spontaneous diffusion into the preformed film) [38,55,56]. Alternatively, a casting deposition method has been used [57]. LbL films assembled from HA/PLL have been widely used for drug loading. High concentration of drugs in the HA/PLL film (hundreds of micromoles) for paclitaxel and diclofenac can be reached and adjusted by the number of deposited layers. The prolonged drug release may take up to some days due to slow molecule diffusion out of the film. Antimicrobial LbL films were reported to be fabricated by deposition of antibiotic (gentamicin sulfate) by integration of the antibiotic as a component of the film using as constituents hydrolytically degradable poly(amino esters) and HA [58]. The film properties can be precisely tuned with regard to the antibiotic loading dosage and release profile at physiological conditions. The release mechanism is based on a combination of spontaneous diffusion out, hydrolytic degradation, and film destruction. For a review on dye-multilayer interactions see [59].

2.2.2. Loading with Nanocontainers

Another option is to load the film with some carriers containing encapsulated molecules. Here we focus on loading of the films with liposomes due to their strong applications in medicine. LbL film fabrication with nanocarriers such as micelles and nanoparticles can be found in the following review [60]. Liposomes are widely accepted as such carriers for biomedical applications [61–64] because of their well-organized compact shell with tunable properties (lipid bilayer membrane), biocompatibility, and size variation over a wide range (from tens of nanometers up to some micrometers for giant vesicles). Liposomes can host not only biomacromolecules with molecular weights typically from a few kDa to tens of kDa but also small molecules. These can be both lipophilic (encapsulation in the vesicle lumen) and hydrophobic (encapsulation into the lipid membrane) small molecules. Surfaces modified with immobilized lipid vesicles are promising candidates for drug delivery and other bioapplications [65–67]. However, liposome disruption and fusion at interfaces is often observed [68,69] making the immobilization in multilayers difficult. It has been demonstrated that highly hydrated polyelectrolyte multilayers made from HA and PLL can host polymer-coated (stabilized) vesicles [70–72] adsorbed by the LbL approach as shown in Figure 1A,B [73–77]. Detailed analysis of the liposome position within the film has shown that they immerse by about half of their size when they come in contact with the surface of the film. This behavior is similar to the behavior of latex particles or polymer microcapsules being in contact with the HA/PLL multilayers [78,79]. Full immersion of vesicles (about 100 nm in diameter) within the film can be achieved just by a few additional LbL coating steps with the same polymers. This may be explained by a difference in the LbL film growth on the top of the immersed vesicles. Polymer diffusion is sterically restricted by the vesicle, and in between the vesicles the polymers

can freely diffuse. The authors have demonstrated that successful embedment of polymer-stabilized vesicles can be achieved by a suitable choice of polymers and lipids used to prepare the films and to formulate the lipid vesicles [73]. The crucial point is to tune an interaction between PLL, liposome, and the outermost polyanion layer of the film. The measured interaction enthalpies between polymers and lipids can be used to predict the assembly of the liposome-containing films [73].

Figure 1. (A) Schematics of HA/PLL films with embedded liposomes assembled by the LbL method. PLL-in blue, HA-in red color; and (B) AFM image of the film with embedded vesicles. The film composition is (PLL/HA)₁₂/PLL-Liposome/HA/PLL/HA. Adopted from [73].



The concept of liposome embedding into the polyelectrolyte multilayers has been used recently to show externally triggered (electrochemically) release of the liposome cargo [80]. This stimulus can be considered as alternative to IR-light as described in the last section of the main text of this review. However, despite high spatial precision (by choosing appropriate electrodes) the electrochemically induced release is rather invasive, because its mechanism is based on the local pH change resulting in destruction of vesicles. Significant changes of the pH value might limit the electrochemical approach for cell biology experiments.

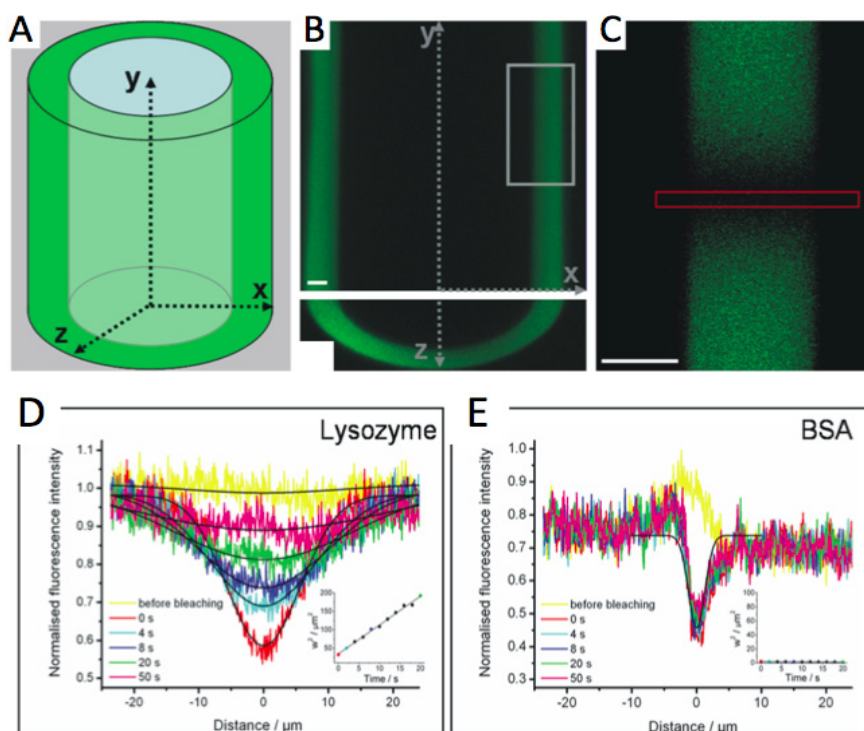
2.2.3. Loading with Proteins and Nucleic Acids

In the following part we will focus on the loading of LbL films with proteins. Proteins and peptides belong to the most used pharmaceuticals. The understanding of the protein interaction with the film constituents will allow controlling the protein release from the film (to a cell). Different bioactive macromolecules e.g., proteins, enzymes, peptides, nucleic acids have been integrated into the LbL film with preserving its biological activity in many cases, [81–83] but sometimes losing its secondary structure if compared to the native structure in solution [84,85]. A large number of studies have been performed for investigation of the interaction of proteins and other biomolecules with the LbL films, see a review for example [13]. The film works as a reservoir with sometimes very high capacity for biomacromolecules. However, there is still no theory describing how the biomacromolecules are embedded within the films and how to predict the loading and their availability from the film to a living cell. This is mostly due to a lack of experimental tools for precise analysis of distribution and behavior (mobility for instance) of the embedded molecules.

2.2.4. Analysis of (Bio)molecule Diffusion and Distribution in the Film

Because of the reason mentioned above, Uhlig and co-workers have developed a method enabling the examination of the multilayer film composition and molecular diffusion in the film with high precision in space and time [86]. CLSM has been adopted for the monitoring of molecular transport in thick (micrometer-sized) multilayer films. A HA/PLL film has been assembled on a cylindrical glass fiber with diameter of 100 μm (Figure 2A,B). The lateral resolution of CLSM is much higher than the vertical one and the film on the fiber has been scanned perpendicularly to the fiber surface. This gives a profile of the film interior (Figure 2B). Not only molecular distribution in the film but also molecular diffusion has been analyzed using fluorescence recovery after photobleaching (FRAP). To measure protein or polymer mobility in the film the authors have bleached a micrometer-sized line along the X-axis and followed the fluorescence recovery from the bleached region.

Figure 2. (A) Schematics of a glass fiber (in blue) coated with (HA/PLL)₂₄ film (in green); (B) CLSM cross-section (x - y scanning) in the middle of a coated fiber (the film in green). In grey frame is the area considered for FRAP experiments; (C) Magnified image of the grey area in B, contrast enhanced image. In red frame is the photobleached area. Scale bars 10 μm ; and (D,E) the mean fluorescence intensity profiles along the whole film as a function of time for lysozyme and BSA, respectively. The insets show the square width at half minimum of the Gaussian w^2 at different time intervals. Adopted from [86].



Using this approach the diffusion of different molecules (proteins as model biomolecules, dextrans, and also small dyes) has been tested (Figure 3A). Based on this study no consistent correlation of diffusion coefficients D with size and charge of tested proteins has been found [86]. Proteins are very mobile in the film, however, do not release fully from the film indicating rather low

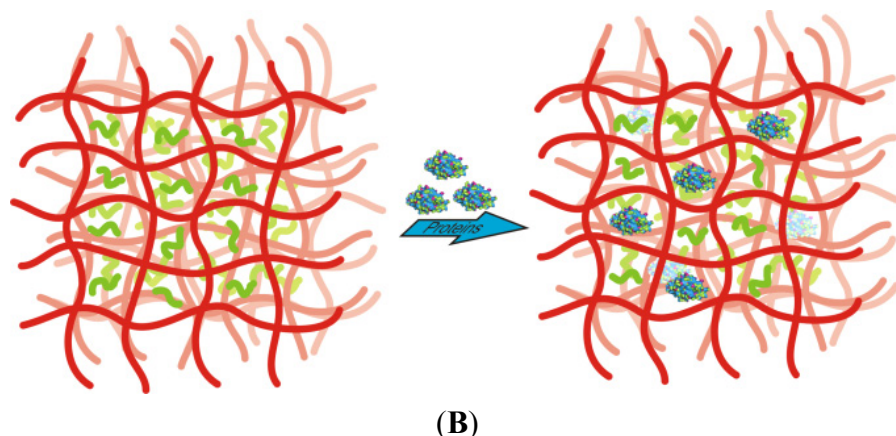
binding enough to keep protein molecules bound to the film matrix. The authors assume that the protein association to and dissociation from the film is rather complex and is not reflected just by protein size and charge. One could expect that the interaction between these molecules will be governed by electrostatics, however, other interactions such as hydrophobic interactions may also play a role. Because of size-independent exclusion of almost uncharged dextrans of 10 and 500 kDa, the authors suggest that the film does not have a distinct permanent mesh size but rather the proteins move inside dynamic pores formed in the immobile matrix of HA and freely diffusing PLL (Figure 3B). This is in line with established models of diffusion of solutes in liquids and melts, where fluctuations should create a free volume into which the solute can jump during a diffusion step. The dynamic pores should have a size in the range of at least 10 nm as it is the size of the largest examined protein (catalase) loaded into the film. The approach developed by Uhlig and co-workers is a strong tool for the analysis of the LbL film structure and molecular dynamics, which is necessary in order to understand the behavior of biomolecules such as proteins in the LbL films in order to control their release and presentation to biological cells [86]. The mechanism of protein–film interaction is not yet clear, but protein retention in the polyelectrolyte complex assembled by the LbL treatment of protein aggregates [87–89] has been demonstrated. This is counterintuitive because inter-polyelectrolyte interaction is supposed to be always stronger than protein–polyelectrolyte interaction due to the higher charge density of linear polyelectrolytes if compared to proteins. However, if one assumes that the multilayers, being non-equilibrium structures should have defects, the protein interactions with free charges in the defects might be a reason.

Figure 3. (A) Table summarizing the main physical-chemical characteristics of (bio)molecules used for analysis of their interaction with the HA/PLL film. Diffusion coefficients D calculated by FRAP are presented as well; and (B) Schematics of the HA/PLL film made of a skeleton of immobile HA (in red) and freely diffusing PLL molecules (in green). The loaded (post-loading) proteins move inside dynamic pores in the skeleton formed due to PLL movement from one position to another. Adopted from [86].

Molecule	M_w [Da]	pI (charge sign)	R_0 [nm]	D [$\mu\text{m}^2 \cdot \text{s}^{-1}$]
Papain	23,400	8.8 (+)	4.2	2.2 ± 0.2
Lysozyme	14,700	11 (+)	1.9	4.4 ± 0.3
Catalase	250,000	5.4 (–)	5.4	3.9 ± 0.3
Lactalbumin	14,200	4.2 (–)	1.7	0.04 ± 0.01
BSA	66,000	5 (–)	3.6	-
Fluorescein	390	(–)		2.1 ± 0.4

(A)

Figure 3. Cont.



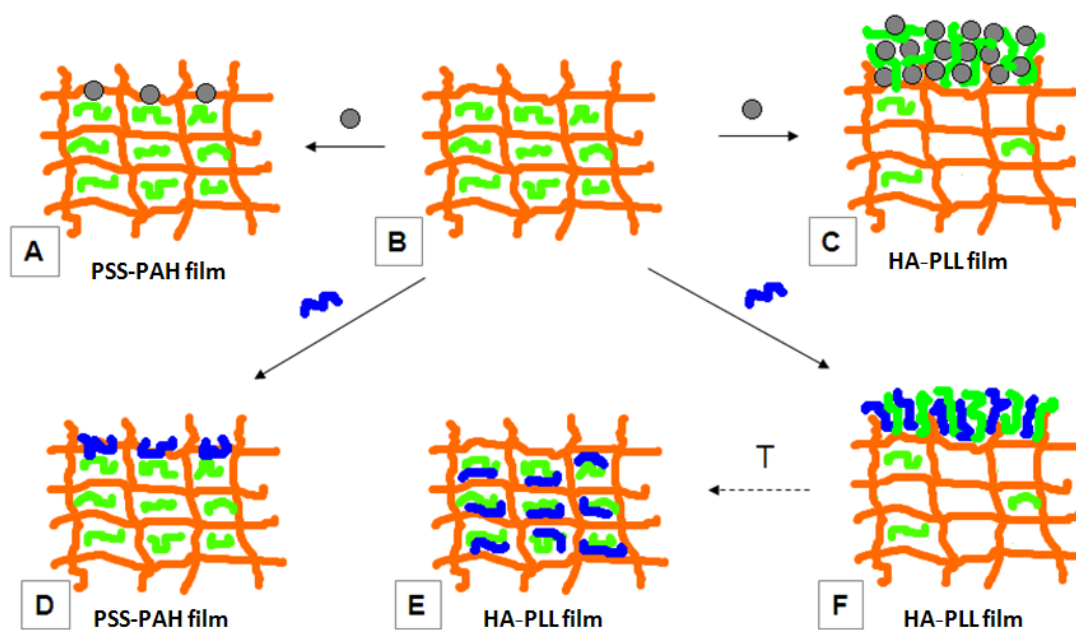
2.2.5. Tailored Polymer Matrices

Composite films containing bioactive molecules (e.g., DNA) and metal nanoparticles may be used for the highly sensitive detection of cell-expressed molecules based on Raman spectroscopy. This is a very strong perspective for the analysis of tissue development and cell biology studies as well as SCA [90–93]. Surface-enhanced Raman spectroscopy (SERS) is developed due to very high signal enhancement by more than 9 orders of magnitude. For SERS the nanoparticles enhance the Raman signal, as has been shown using spherical inorganic carbonate matrices coated with polyelectrolyte multilayers [94]. To understand the loading mechanism and structure of the composite LbL films, two kinds of LbL films (or PSS/PAH and HA/PLL) have been tested for interaction with negatively charged DNA and gold nanoparticles [25]. A scheme of the interaction is presented in Figure 4. These films exhibit low and high mobility of the used polycations-PAH and PLL, respectively.

The interaction of gold nanoparticles or DNA with the PSS/PAH film leads to their adsorption at the surface of the film driven by complex formation with the chains of immobile PAH (outermost layer) (Figure 4(B→A, B→D)). However, for HA/PLL films faster diffusing PLL molecules are transported from the film internal volume to its surface to make more contacts with the adsorbing DNA or the nanoparticles (Figure 4(B→C, B→F)). Diffusion of DNA or gold nanoparticles [25,36] into the whole film is, however, restricted due to the strong interaction with PLL. There is an excess of PLL amino groups in the HA/PLL films, and as found in literature there are two times more free amino groups compared to the carboxylic groups of HA [95]. This could cause a high mobility of PLL and the described above doping effect. The authors suppose that a high content of free amino groups and a high mobility of PLL allows embedding of DNA. For example Srivastava [96] has reported accumulation of quantum dots with sizes of a few nanometers in the exponentially growing LbL film. The authors in [25] also showed that the PLL doping is responsible for accumulation of high amount of negatively charged DNA or nanoparticles, but not for the salting out of DNA molecules due to high salt content in the film (high number of counterions). For this the film with pre-adsorbed nanoparticles has been brought into contact with PLL molecules or salt and later the new portion of nanoparticles has been added. In case of additional PLL doping nanoparticles started to adsorb again. Both nanoparticles and DNA form micrometer-sized agglomerates at the film surface that is explained by the authors by a charge compensation in agglomerates till the charges on the agglomerate edges do not

“fill” each other (no electrostatic repulsion). The agglomerates contain PLL molecules as has been proven using fluorescently labeled PLL [25].

Figure 4. A scheme representing the interaction of the LbL film (**B**) made of HA (orange network) and PLL (in green) with metal nanoparticles (grey spheres, **B**→**A** and **B**→**C**) and DNA (in blue, **B**→**D** and **B**→**F**). DNA or the nanoparticles can be accumulated in high amount because of interaction with PLL molecules “transported” from the film interior to the surface. DNA diffusion into the HA/PLL film is induced by heating (70 °C, **F**→**E**). (Adapted with permission from [25]. Copyright 2009 American Chemical Society).



The very high loading capacity for DNA and gold nanoparticles for HA/PLL films (about 1%–2% and 100% of the mass of PLL in the film, respectively) can be attributed just to the PLL doping to the film surface. It has also been shown that the last layer of the film plays a role for nanoparticle–film interaction, supporting the doping mechanism described above. In case of like charges of particles and the last deposited layer (HA) the amount of adsorbed particles was less, and less aggregation has been observed [97]. At the same time the amount of adsorbed particles and DNA was about an order of magnitude lower for the film with immobile polymers-PSS/PAH film-if compared to the HA/PLL film [25].

The knowledge of the interaction between gold nanoparticles within the film is important to control the optical properties of the film. The peak intensity of UV/vis spectra (absorption maximum at 520 nm) of PSS/PAH films with embedded nanoparticles is much lower than the one for HA/PLL films doped with Au-NPs [25]. The HA/PLL film resorbs much more nanoparticles and the absorption spectrum shows a long shoulder towards the infra-red (IR) region [25]. This indicates that the inter-particle interaction results in an aggregation of Au-NPs and plasmon coupling. This opens perspectives for biologically relevant applications, because IR-light is more penetrative to tissues and less harmful for cells [41].

Thus, the HA/PLL film is a matrix providing a high amount of material due to its reservoir properties driven by PLL doping. The diffusion of the embedded molecules is of high importance,

because the release or/and the molecular presentation from the film as driven by light exposure would be a mechanism of light-triggered treatment. It has been demonstrated that DNA diffusion in the film can be stimulated by temperature [25]. An analysis of CLSM stack profiles for distribution of PLL and DNA in the film as a function of temperature (heating up to 70 °C) has been done. After heating the profiles of DNA and PLL almost coincide. This without doubts indicates temperature-mediated diffusion. All DNA molecules stay in the film as shown by consideration of the integral fluorescence from the DNA stack profiles. It is of note that the HA/PLL film is stable against heating to rather high temperatures (up to 50 °C) [73].

Thus, the improvement of the molecular mobility in the HA/PLL film triggered by temperature may be used to release molecules or present them to the film surface (for instance to biological cells). Light has been adopted for external stimulation of complex HA/PLL films containing DNA and nanoparticles aiming at light-triggered release. This issue is addressed in the last section of this review.

3. Cell Patterning by LbL Films

Formation of a tissue is regulated by a variety of biological factors such as cell–ECM interactions, intercellular communication, and presentation of soluble factors. More details on biological aspects of cell–matrix interaction including interaction with cell adhesion membrane proteins can be found in the following publications [26–28]. Recapitulation of such interactions is a key in tissue engineering applications. For this purpose, manipulation the cell microenvironment has been achieved by surface patterning with a certain cell-adhesive or cell-repellent molecules or topological features which lead to formation of cellular patterns [98]. The localization of cells or single cells on a surface is of crucial importance to achieve SCA for adherent cells, and the polyelectrolyte multilayers have successfully been utilized for control over cellular organization (location) on a solid surface. The main approach of the technique-sequential polymer deposition resulting in surface overcharging-has been used to switch the surface properties from cell repellent to cell adhesive. For this purpose, two polymers with opposite characteristics with respect to cellular adhesion are deposited. The model films made of ionic biopolymers such as HA/PLL or HA/collagen films have been shown to be perfect candidates for this application [99,100]. Adsorption of a thin layer of HA leads to the cell repulsive surface. Subsequent adsorption of PLL results in a switch of the surface properties and cellular adhesion. Thus, by using well-established soft lithography approaches a cell co-culture has been formed on a 2D surface (Figure 5).

The approach described above is shown for coating of a thin surface layer with a monolayer of another polymer. The multilayer film reservoir properties are important for loading of substantial amounts of bioactive molecules. The reservoir capacity depends on the film thickness, and for thin films (usually tens of nanometers or less) the loading capacity is rather low. This is why patterned thin multilayers are not attractive for delivery of biomolecules from the film but can be effectively used to pattern biological cells. At the same time the LbL films made from biopolymers are growing in many cases exponentially and can reach micrometer dimensions rather fast. However, they are hydrated (soft) and as a result cell-repellent [22,101]. More details on a relation of physical-chemical properties of the LbL films to cellular response one can find in a comprehensive review [22]. To make them cell-adhesive the soft films have been either capped with stiffer multilayers [38] or cross-linked chemically [32,35,55]. Alternatively, film composition (e.g., polymer length) may be used to tune

cell–film interaction [102]. Recently, surface capping of the films with metal nanoparticles has been shown as a way to make the soft films cell-friendly but to keep the main part of the film intact to keep the reservoir properties of the film [36]. The latter is not the case for covalent chemical crosslinking [32,35,55].

An alternative and more advantageous approach for making the soft LbL films cell-friendly is to prepare thick patterned films. In this case, the film properties are not affected neither chemically nor physically [12,101,103]. Such a novel method, based on the assembly of soft films using a microfluidic platform for selective cell growth, has been recently introduced [39]. As can be seen from Figure 6, a microfluidic channel from polydimethylsiloxane (PDMS) with microstructured geometry has been used. The polymers PLL and HA were deposited into the microchannels to form multilayers in between the defined features of the PDMS stamp (Figure 6A). Peeling off the PDMS stamp from the glass under complete immersion in buffer results in patterning of the formed soft film. Afterwards the cells have been seeded and grown exclusively in the patterned areas (Figure 6A).

Figure 5. (I) Schematics of design of the co-culture system by a combination of capillary force lithography and the LbL technique. A PDMS mold has been placed onto a spin-coated thin HA layer followed by receding of the HA layer under the mold void space. Fibronectin has been deposited onto the patterned HA layer followed by selective adhesion of cells to the pattern regions. Subsequently, the HA layer has been coated with collagen that allows for selective adhesion of a secondary cell type; and (II) (A)–Patterned cell culture and co-culture on HA-collagen surface. Fibronectin coated patterns have been occupied by primary cells–murine embryonic stem cells (A) and AML12 murine hepatocytes (B) after 8 h incubation time. Fluorescently stained co-culture of primary cells and NIH-3T3 fibroblasts adheres to the HA-collagen-coated regions between the patterned circles (C and D). (Adapted with permission from [99]. Copyright 2006 Elsevier).

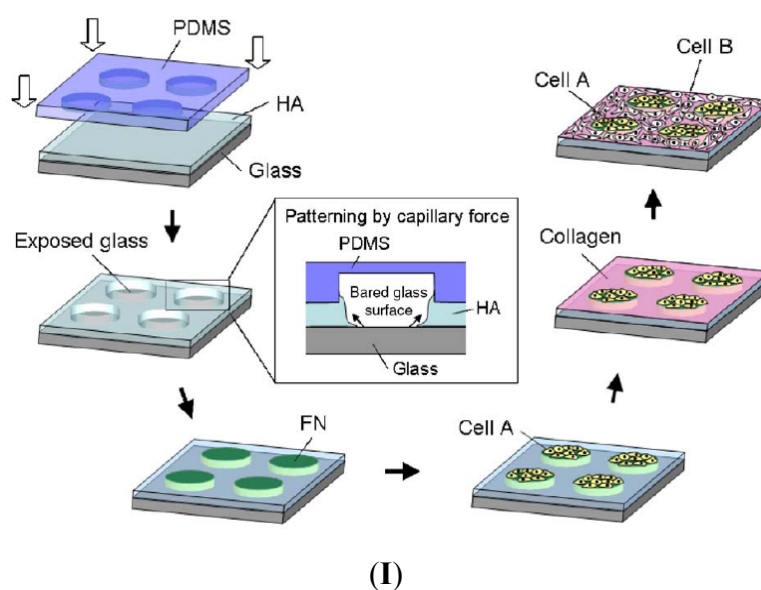


Figure 5. Cont.

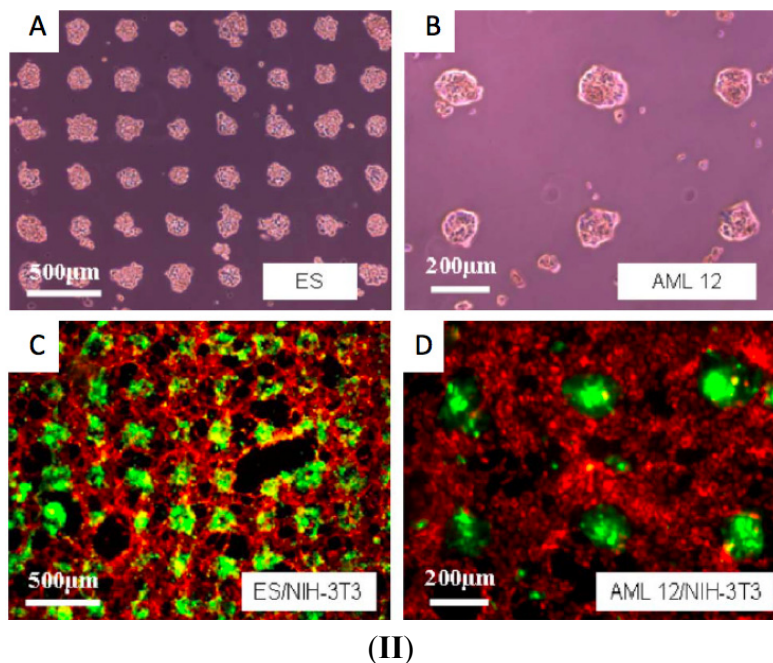
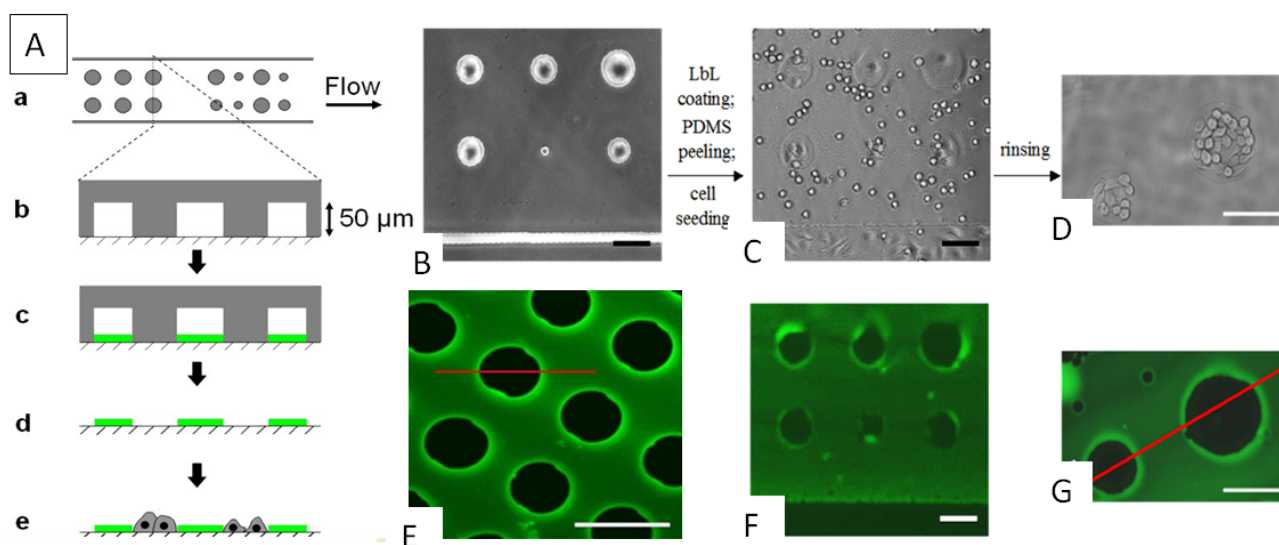


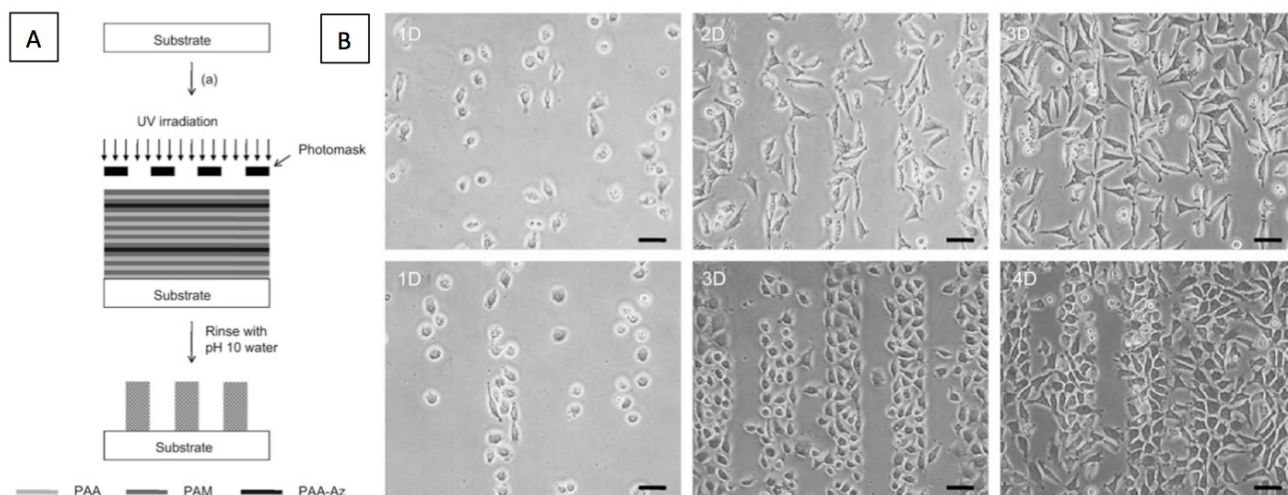
Figure 6. (A) Schematics of the patterning of $(HA/PLL)_{24}$ soft film in a microfluidic channel. (a) The top-view of channel region with spherical structures; (b) Cross-section of the region indicated by dotted lines (side view); the glass is at the bottom and PDMS pillars on the glass; (c) Multilayer deposition in the empty regions in the channel. (d) Deposited patterned LbL film after PDMS stamp removal; (e) Selective cell growth on uncoated (patterned) film areas; and (B) Phase-contrast image of the channel before LbL deposition; (C) Phase-contrast image of the region after film assembly followed by PDMS stamp removal and subsequent seeding of L929 fibroblasts (2 h incubation); (D) Phase-contrast image of zoomed region of the channel after 6 h pre-incubation followed by cell rinsing; (E) CLSM image showing the patterned film before PDMS removal; and (F,G) Fluorescence images of (C) and (D), respectively. The scale bar is 100 μm in all cases. Adopted from [39].



The HA/PLL films deposited at the same conditions by the conventional technique (dipping) and the films formed by microfluidics are similar in terms of mechanical properties meaning that material properties of the assembled film are preserved during deposition in microchannels and also after peeling off the PDMS stamp. Microfluidics, however, significantly improves molecular transport to the film interface during deposition, thus stimulating polymer diffusion into the film resulting in significantly faster film growth [104]. Patterned regions are free of polymer as can be concluded by comparing the fluorescent signal from the patterned regions and from the region outside the channel where the film has not been assembled (Figure 6F). By comparison of the phase contrast and fluorescence images one can conclude that the sizes of the various (tuned by manufacture conditions) stamp features are reproduced relative to each other (Figure 6D,G). Cell (L929 fibroblasts) seeding onto the multilayer film after PDMS stamp removal results in highly selective cellular adhesion. The cells that sediment onto the non-patterned regions do not spread well and can be easily washed away by rinsing (Figure 6C,D). The adherent cells in contrast remain within their confinement for long time indicating a high stability of the patterned films.

An alternative method to pattern LbL films is photolithography when the film is crosslinked by UV light irradiation and the non-crosslinked areas are washed away at conditions where the film is unstable [105]. Figure 7 shows the approach schematics (Figure 7A) and cell patterns (Figure 7B). For the photolithography approach, a change of the chemical composition of the film during the crosslinking process and exposure to conditions of the film decomposition are not favorable for biological applications, especially if a bioactive molecule is loaded before the film patterning.

Figure 7. (A) Schematics of fabrication of an LbL film patterned by photolithography: the film is deposited on a solid substrate followed by UV-light irradiation through the mask (film crosslinking) and washing away of the non-irradiated film areas; and (B) phase contrast images of L929 fibroblasts cultured on the patterned (poly(acrylic acid)/polyacrylamide)_x or (PAA/PAM)_x film ($x = 5$ and 20 for upper and lower rows, respectively). PAA-Az is PAA, conjugated with 4-azi-doaniline. Incubation time (days, D) is shown in the left upper corner of the images. Scale bar is $50\ \mu\text{m}$. (Adapted with permission from [105]. Copyright 2009 Elsevier).



The patterned films such as HA/PLL films described above have micrometer thickness, similar to the dimensions of adherent cells; the patterned films may thus be perceived as 3D-structures by the cells. Therefore, this novel approach for fabricating micropatterned LbL films may serve in future as 3D coating for advanced cell culturing applications. The patterned micrometer-sized films may work as reservoirs for biomolecules of interest as has been described earlier. From a fundamental point of view the prepared patterned films with highly selective cell adhesion may be used as artificial niches for ECM study and stem cell biology as well as for single-cell manipulations. A combination of stimuli-sensitive composite films (such as DNA and nanoparticles containing films as described in the previous section) with film patterning may pave a way for applications focusing on the level of a single cell. In the next section we will focus on external (IR-light) stimulation of multilayers for controlled release as an attractive feature for SCA allowing improving the precision for delivery of the released molecules in space and time.

4. Light-Triggered Delivery

In this chapter we focus only on light-responsive multilayer films as an “on demand” delivery system. Despite a variety of materials responsive to external stimuli have been developed allowing various remote stimulation approaches, [106] we consider just one stimulus, light, that has significant advantage in focusing, control over intensity as well as non-invasive character from the biological point of view (IR-light). The stability of the liposomes trapped in the LbL film (described above) should be considered if this composite film is going to be used for localized externally triggered release. This localized release can be pursued if liposomes are immobilized in the HA/PLL film [74,107]. Vesicle cargos (model dye carboxyfluorescein (CF) or silver nitrate as antibacterial agent) are kept in the vesicles if the lipid membrane is in a solid state. This is the case below the phase transition temperature which is 41 °C for vesicles made of 1,2-dipalmitoyl-*sn*-glycero-3-phosphocholine, 1,2-dipalmitoyl-*sn*-glycero-3-phospho-*rac*-(1-glycerol), and cholesterol [74,107]. However, the molecules are extensively released if the temperature is above 41 °C. The release is induced by an increase in permeability of the lipid membrane but not by a response of the film to a temperature increase which may lead to a vesicle rupture [74]. At the same time the permeability of the liposome membrane can be achieved by local heating above the phase transition temperature induced by light irradiation (Figure 8B) [108]. The heating is due to conversion into heat of light energy absorbed by single or aggregated gold nanoparticles, which work as “hot spots” (Figure 8A). Thus, light-stimulated release from liposome-containing LbL films might be considered for light-triggered delivery providing a control over film-mediated delivery of bioactive compounds on demand.

Let us now consider light-triggered release from the film loaded directly with biomolecules. As has been shown in the previous section, film heating can affect the film composition inducing enhancement of DNA transport into the film. Adsorption of macromolecules (DNA) at the film surface depends on the interaction with the doped PLL and an interruption of this interaction by local heating resulting in higher DNA mobility and even in release of DNA molecules from the film as depicted in Figure 9B,C [25,109]. DNA is released over a distance (tens of micrometers) far away from the heating place showing that most probably the DNA–PLL interaction can be affected over a distance, where temperature increase is not high or the temperature is ambient temperature [25].

Figure 8. (A) Scheme of a complex of liposomes with gold nanoparticles (either single or nanoparticle aggregates). Liposome cargo is released if the temperature is above the lipid phase transition temperature; and (B) CLSM fluorescence images before and after illumination of a complex of CF-filed liposome with gold nanoparticles. The scale bar is 10 μm . (Adapted with permission from [108]. Copyright 2009 John Wiley and Sons).

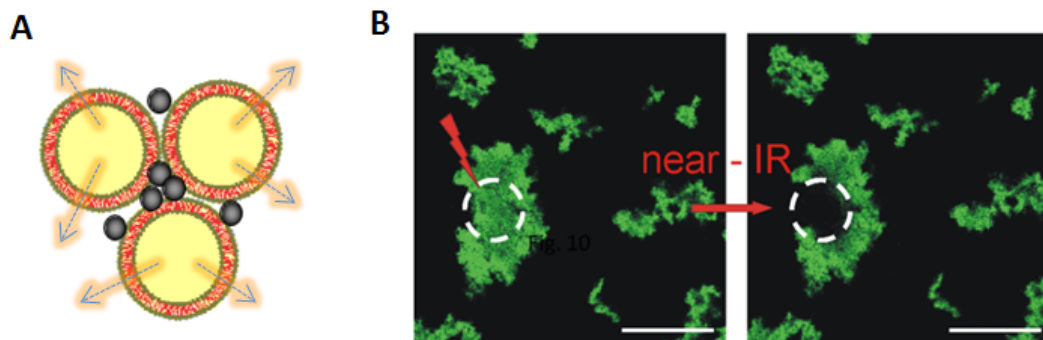
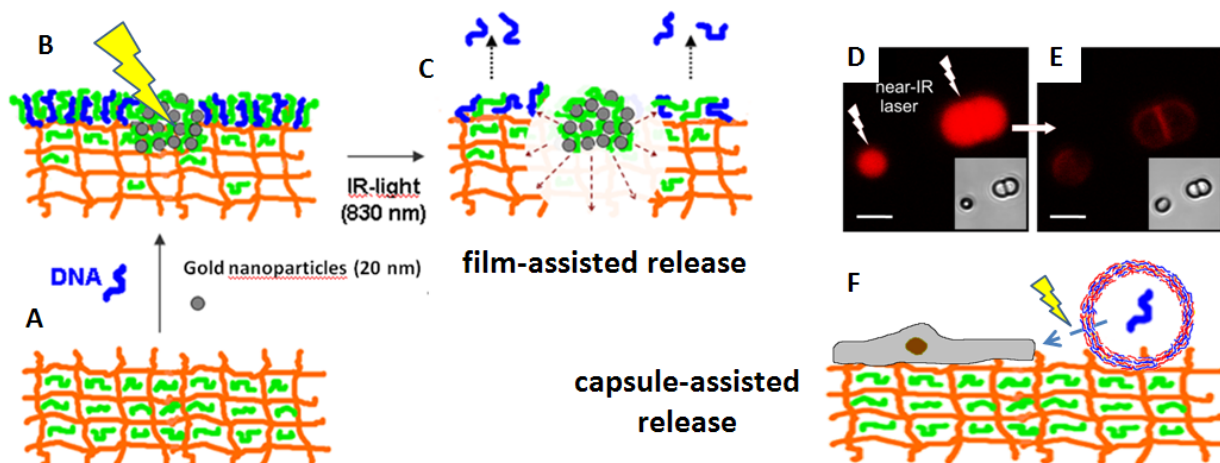


Figure 9. Schematics of the proposed mechanism of light-triggered DNA release from HA/PLL multilayers. (A,B) loading of the HA/PLL film (HA in orange, PLL in green) with gold nanoparticles and DNA (in blue); (B,C) thermal decomposition of the film around nanoparticle aggregates upon light irradiation resulting in distortion (weakening) of the interaction between DNA and the doped PLL and, as a result, in DNA release from the film. CLSM images of nanoparticle coated (poly(diallyldimethylammonium chloride)/PSS)₄ microcapsules loaded into the (PLL/HA)₂₄/PLL film before (D) and after (E) light irradiation during 1s. Light power is 20 mW, wavelength is 830 nm. The scale bar is 1 μm ; and (F) Scheme of light-triggered biomolecule release from microcapsules to a biological cell, both located on the film. Adopted from [25].



The authors suggest a mechanism of long-distance activation by IR-light. A decrease in PLL fluorescence from the film is evidence of the local heating of the HA/PLL films when absorbed light energy is converted to heat in the vicinity of the nanoparticles. PLL molecules most probably get pushed out of the film. The film outside the affected area is not decomposed after light irradiation at a power above 20 mW (wavelength 830 nm) that could be due to temperature-mediated crosslinking between PLL and HA, as has been shown in literature at a temperature above 100 $^{\circ}\text{C}$ [110,111].

However, DNA has been released on a distance of tens of micrometers from the heated aggregates. The temperature profile for the light-affected nanoparticle aggregates is rather sharp and the temperature close to ambient temperature is already reached at a distance of a few ten nanometers from the aggregates [112]. This allows one to guess that DNA molecules are released from the film surface because the interaction of DNA with the film (with oppositely charged PLL in the film) becomes weaker. In addition, the PLL concentration in the film is reduced due to later PLL diffusion from the whole film towards the light affecting area. Thus, long-distance effects might be possible.

A multilayer film with embedded biomolecule-loaded carriers (capsules) presents an alternative delivery carrier where the loaded molecule release is triggered by a change in the permeability of the carrier (capsule) shell [25,113,114]. Reservoir properties of the HA/PLL film allow the embedding of small and rather large objects, also large carriers such as microcapsules [25,74,78,79,97]. Light-sensitive multilayer microcapsules modified with gold nanoparticles have been embedded into the HA/PLL film by spontaneous loading [25]. These capsules do not adhere to the PSS/PAH film (can easily be washed out) but once adsorbed on the HA/PLL film the capsules are immobilized which is explained by the PLL doping mechanism as described above. In addition to the doping effect of PLL, one has also to consider polyelectrolyte exchange between the capsule and the film because both are made of polyelectrolyte multilayers [115]. Afterwards the capsules were irradiated by the laser beam resulting in a local heating of the capsule shell followed by the shell decomposition and subsequent release of the encapsulated molecules (fluorescently labeled dextran). Figure 9D shows CLSM images of the capsules on the film before and after the light-mediated release. It is of note that the irradiated capsule keeps spherical shape after the light influence which demonstrates only local shell decomposition (Figure 9D). One drawback of encapsulation into multilayer capsules is that a significant amount of encapsulated molecules is absorbed by the capsule shell due to the high capacity of the multilayer shell [116]. Another limitation is that the encapsulation is in many cases achieved by temperature-mediated (above 50 °C) capsule shrinkage that leads to capture of the biomolecules inside the capsule. Alternatively, encapsulation has been achieved by using biologically non-relevant compounds, for instance HF or organic solvents [117–119]. These compounds are necessary to eliminate a core during an encapsulation process. The improvement of both encapsulation efficiency and retention of bioactivity might be achieved by using porous CaCO₃ particles allowing loading of large amount of proteins by means of physical or chemical crosslinking at mild conditions [120–128].

5. Conclusions and Perspectives

An analysis of literature suggests that the LbL-assembled polyelectrolyte multilayers are an attractive platform for SCA. The main criteria for their utilization are established. These include cell patterning as well as loading and controlled release of bioactive molecules into/from the film. Cell patterning by the LbL films has been demonstrated using various approaches. Loading of biomolecules into the LbL films has also been demonstrated. Most probably the interaction is of electrostatic origin and based on the formation of ion pairs between free groups of the polyelectrolyte backbone and protein or other charged biomolecules. Presentation of protein molecules (e.g., growth factors) to a cell by a diffusion through multilayers better mimics a natural way of transport of soluble signal molecules in the ECM. However, there is still no theory describing protein behavior in polyelectrolyte

multilayers. This, to our opinion, should be considered in the near future, but it will be difficult to generalize, because each protein has an individual structure and function. Therefore, the best strategy appears to be to keep the interactions sufficiently weak not to affect a protein.

The controlled release of biomolecules from the films at conditions applicable for cellular studies (physiological conditions, cell culture medium) has not been well studied. This topic should be considered more in future. However, as has been shown, a combination of light-sensitive multilayer capsules with the multilayer films is a good candidate for controlled release [129]. At the same time the challenges for such composite films concern not only the films but also the carriers for biomolecules—the capsules. The low encapsulation of proteins in the capsules due to the large capacity of the capsule polymer shell should be overcome [116]. Another aspect in the encapsulation process is the biological activity of the encapsulated molecules. The methods used up to now include the utilization of organic solvents, HF, or high temperature for the encapsulation into the multilayer capsules. In future more mild encapsulation conditions should be employed, e.g., encapsulation based on CaCO₃ templating.

Acknowledgment

D. Volodkin thanks A. von Humboldt Foundation for support (Sofja Kovalevskaja Program).

Conflicts of Interest

The authors declare no conflict of interest.

References

1. Wang, D.; Bodovitz, S. Single cell analysis: The new frontier in “omics”. *Trends Biotechnol.* **2010**, *28*, 281–290.
2. Fritzsche, F.S.O.; Dusny, C.; Frick, O.; Schmid, A. Single-cell analysis in biotechnology, systems biology, and biocatalysis. *Annu. Rev. Chem. Biomol. Eng.* **2012**, *3*, 129–155.
3. Graf, T.; Stadtfeld, M. Heterogeneity of embryonic and adult stem cells. *Cell Stem Cell* **2008**, *3*, 480–483.
4. Kleparnik, K.; Foret, F. Recent advances in the development of single cell analysis—A review. *Anal. Chim. Acta* **2013**, *800*, 12–21.
5. Chao, T.C.; Ros, A. Microfluidic single-cell analysis of intracellular compounds. *J. R. Soc. Interface* **2008**, *5*, S139–S150.
6. Decher, G. Fuzzy nanoassemblies: Toward layered polymeric multicomposites. *Science* **1997**, *277*, 1232–1237.
7. Decher, G.; Hong, J.-D. Buildup of ultrathin multilayer films by a self-assembly process: I. consecutive adsorption of anionic and cationic bipolar amphiphiles. *Makromol. Chem.* **1991**, *46*, 321–327.
8. Peyratout, C.S.; Dahne, L. Tailor-made polyelectrolyte microcapsules: From multilayers to smart containers. *Angew. Chem. Int. Ed.* **2004**, *43*, 3762–3783.

9. Ariga, K.; Hill, J.P.; Li, Q. Layer-by-layer assembly as a versatile bottom-up nanofabrication technique for exploratory research and realistic application. *Phys. Chem. Chem. Phys.* **2007**, *9*, 2319–2340.
10. Wang, Y.J.; Hosta-Rigau, L.; Lomas, H.; Caruso, F. Nanostructured polymer assemblies formed at interfaces: Applications from immobilization and encapsulation to stimuli-responsive release. *Phys. Chem. Chem. Phys.* **2011**, *13*, 4782–4801.
11. Gero Decher, J.B.S. *Multilayer Thin Films: Sequential Assembly of Nanocomposite Materials*, 2nd ed.; Wiley-VCH: Weinheim, Germany, 2012.
12. Tang, Z.; Wang, Y.; Podsiadlo, P.; Kotov, N.A. Biomedical applications of layer-by-layer assembly: From biomimetics to tissue engineering. *Adv. Mater.* **2006**, *18*, 3203–3224.
13. Lavallo, P.; Voegel, J.C.; Vautier, D.; Senger, B.; Schaaf, P.; Ball, V. Dynamic aspects of films prepared by a sequential deposition of species: Perspectives for smart and responsive materials. *Adv. Mater.* **2011**, *23*, 1191–1221.
14. Sukhishvili, S.A. Responsive polymer films and capsules via layer-by-layer assembly. *Curr. Opin. Colloid Interface Sci.* **2005**, *10*, 37–44.
15. Volodkin, D.; Skirtach, A.; Mohwald, H. LbL films as reservoirs for bioactive molecules. In *Bioactive Surfaces*; Borner, H.G., Lutz, J.F., Eds.; Springer-Verlag Berlin: Berlin, Germany, 2011; Volume 240, pp. 135–161.
16. Volodkin, D.V.; Mohwald, H. Polyelectrolyte multilayers for drug delivery. In *Encyclopedia of Surface and Colloid Science*; Somasundaran, P., Ed.; Taylor & Francis Group, LLC: Abingdon, UK, 2009; Volume 1, p. 14.
17. Delcea, M.; Mohwald, H.; Skirtach, A.G. Stimuli-responsive LbL capsules and nanoshells for drug delivery. *Adv. Drug Deliv. Rev.* **2011**, *63*, 730–747.
18. De Geest, B.G.; Sukhorukov, G.B.; Mohwald, H. The pros and cons of polyelectrolyte capsules in drug delivery. *Exp. Opin. Drug Deliv.* **2009**, *6*, 613–624.
19. De Geest, B.G.; Sanders, N.N.; Sukhorukov, G.B.; Demeester, J.; de Smedt, S.C. Release mechanisms for polyelectrolyte capsules. *Chem. Soc. Rev.* **2007**, *36*, 636–649.
20. Hirano, Y.; Mooney, D.J. Peptide and protein presenting materials for tissue engineering. *Adv. Mater.* **2004**, *16*, 17–25.
21. Crouzier, T.; Ren, K.; Nicolas, C.; Roy, C.; Picart, C. Layer-by-layer films as a biomimetic reservoir for rhBMP-2 delivery: Controlled differentiation of myoblasts to osteoblasts. *Small* **2009**, *5*, 598–608.
22. Boudou, T.; Crouzier, T.; Ren, K.; Blin, G.; Picart, C. Multiple functionalities of polyelectrolyte multilayer films: new biomedical applications. *Adv. Mater.* **2010**, *22*, 441–467.
23. Jewell, C.M.; Lynn, D.M. Multilayered polyelectrolyte assemblies as platforms for the delivery of DNA and other nucleic acid-based therapeutics. *Adv. Drug Deliv. Rev.* **2008**, *60*, 979–999.
24. Jewell, C.M.; Zhang, J.; Fredin, N.J.; Lynn, D.M. Multilayered polyelectrolyte films promote the direct and localized delivery of DNA to cells. *J. Control. Release* **2005**, *106*, 214–223.
25. Volodkin, D.V.; Madaboosi, N.; Blacklock, J.; Skirtach, A.G.; Mohwald, H. Surface-supported multilayers decorated with bio-active material aimed at light-triggered drug delivery. *Langmuir* **2009**, *25*, 14037–14043.

26. Lutolf, M.P.; Hubbell, J.A. Synthetic biomaterials as instructive extracellular microenvironments for morphogenesis in tissue engineering. *Nat. Biotech.* **2005**, *23*, 47–55.
27. Stevens, M.M.; George, J.H. Exploring and engineering the cell surface interface. *Science* **2005**, *310*, 1135–1138.
28. Guillame-Gentil, O.; Semenov, O.; Roca, A.S.; Groth, T.; Zahn, R.; Voros, J.; Zenobi-Wong, M. Engineering the extracellular environment: Strategies for building 2D and 3D cellular structures. *Adv. Mater.* **2010**, *22*, 5443–5462.
29. Üzümlü, C.; Hellweg, J.; Madaboosi, N.; Volodkin, D.V.; von Klitzing, R. Growth behavior and mechanical properties of PLL/HA multilayer films studied by AFM. *Beilstein J. Nanotechnol.* **2012**, *3*, 778–788.
30. Picart, C.; Lavalle, P.; Hubert, P.; Cuisinier, F.J.G.; Decher, G.; Schaaf, P.; Voegel, J.-C. Buildup mechanism for poly(L-lysine)/hyaluronic acid films onto a solid surface. *Langmuir* **2001**, *17*, 7414–7424.
31. Semenov, O.V.; Malek, A.; Bittermann, A.G.; Voros, J.; Zisch, A.H. Engineered polyelectrolyte multilayer substrates for adhesion, proliferation, and differentiation of human mesenchymal stem cells. *Tissue Eng. A* **2009**, *15*, 2977–2990.
32. Richert, L.; Lavalle, P.; Payan, E.; Shu, X.Z.; Prestwich, G.D.; Stoltz, J.-F.; Schaaf, P.; Voegel, J.-C.; Picart, C. Layer by layer buildup of polysaccharide films: Physical chemistry and cellular adhesion aspects. *Langmuir* **2004**, *20*, 448–458.
33. Francius, G.; Hemmerlé, J.; Ball, V.; Lavalle, P.; Picart, C.; Voegel, J.-C.; Schaaf, P.; Senger, B. Stiffening of soft polyelectrolyte architectures by multilayer capping evidenced by viscoelastic analysis of AFM indentation measurements. *J. Phys. Chem. C* **2007**, *111*, 8299–8306.
34. Schneider, A.; Francius, G.; Obeid, R.; Schwinté, P.; Hemmerlé, J.; Frisch, B.; Schaaf, P.; Voegel, J.-C.; Senger, B.; Picart, C. Polyelectrolyte multilayers with a tunable young's modulus: Influence of film stiffness on cell adhesion. *Langmuir* **2005**, *22*, 1193–1200.
35. Ren, K.; Crouzier, T.; Roy, C.; Picart, C. Polyelectrolyte multilayer films of controlled stiffness modulate myoblast cell differentiation. *Adv. Funct. Mater.* **2008**, *18*, 1–12.
36. Schmidt, S.; Madaboosi, N.; Uhlig, K.; Köhler, D.; Skirtach, A.; Duschl, C.; Möhwald, H.; Volodkin, D.V. Control of cell adhesion by mechanical reinforcement of soft polyelectrolyte films with nanoparticles. *Langmuir* **2012**, *28*, 7249–7257.
37. Podsiadlo, P.; Tang, Z.; Shim, B.S.; Kotov, N.A. Counterintuitive effect of molecular strength and role of molecular rigidity on mechanical properties of layer-by-layer assembled nanocomposites. *Nano Lett.* **2007**, *7*, 1224–1231.
38. Vodouhê, C.; le Guen, E.; Mendez Garza, J.; Francius, G.; Déjugnat, C.; Ogier, J.; Schaaf, P.; Voegel, J.-C.; Lavalle, P. Control of drug accessibility on functional polyelectrolyte multilayer films. *Biomaterials* **2006**, *27*, 4149–4156.
39. Madaboosi, N.; Uhlig, K.; Schmidt, S.; Jager, M.S.; Möhwald, H.; Duschl, C.; Volodkin, D.V. Microfluidics meets soft layer-by-layer films: selective cell growth in 3D polymer architectures. *Lab Chip* **2012**, *12*, 1434–1436.
40. Ariga, K.; McShane, M.; Lvov, Y.M.; Ji, Q.M.; Hill, J.P. Layer-by-layer assembly for drug delivery and related applications. *Exp. Opin. Drug Deliv.* **2011**, *8*, 633–644.
41. Weissleder, R. A clearer vision for *in vivo* imaging. *Nat. Biotech.* **2001**, *19*, 316–317.

42. Ntziachristos, V. Going deeper than microscopy: The optical imaging frontier in biology. *Nat. Methods* **2010**, *7*, 603–614.
43. Takayama, S.; Ostuni, E.; LeDuc, P.; Naruse, K.; Ingber, D.E.; Whitesides, G.M. Laminar flows-Subcellular positioning of small molecules. *Nature* **2001**, *411*, 1016.
44. Schonhoff, M. Self-assembled polyelectrolyte multilayers. *Curr. Opin. Colloid Interface Sci.* **2003**, *8*, 86–95.
45. Von Klitzing, R. Internal structure of polyelectrolyte multilayer assemblies. *Phys. Chem. Chem. Phys.* **2006**, *8*, 5012–5033.
46. Volodkin, D.; von Klitzing, R. Competing mechanisms in polyelectrolyte multilayer formation and swelling: Polycation–polyanion pairing vs. polyelectrolyte–ion pairing. *Curr. Opin. Colloid Interface Sci.* **2014**, *19*, 25–31.
47. Nazaran, P.; Bosio, V.; Jaeger, W.; Anghel, D.F.; von Klitzing, R. Lateral mobility of polyelectrolyte chains in multilayers. *J. Phys. Chem. B* **2007**, *111*, 8572–8581.
48. Lavallo, P.; Picart, C.; Mutterer, J.; Gergely, C.; Reiss, H.; Voegel, J.-C.; Senger, B.; Schaaf, P. Modeling the buildup of polyelectrolyte multilayer films having exponential growth. *J. Phys. Chem. B* **2004**, *108*, 635–648.
49. Ghostine, R.A.; Markarian, M.Z.; Schlenoff, J.B. Asymmetric growth in polyelectrolyte multilayers. *J. Am. Chem. Soc.* **2013**, *135*, 7636–7646.
50. Wong, J.E.; Zastrow, H.; Jaeger, W.; von Klitzing, R. Specific ion vs. electrostatic effects on the construction of polyelectrolyte multilayers. *Langmuir* **2009**, *25*, 14061–14070.
51. Laugel, N.; Betscha, C.; Winterhalter, M.; Voegel, J.-C.; Schaaf, P.; Ball, V. Relationship between the growth regime of polyelectrolyte multilayers and the polyanion/polycation complexation enthalpy. *J. Phys. Chem. B* **2006**, *110*, 19443–19449.
52. Doodoo, S.; Steitz, R.; Laschewsky, A.; von Klitzing, R. Effect of ionic strength and type of ions on the structure of water swollen polyelectrolyte multilayers. *Phys. Chem. Chem. Phys.* **2011**, *13*, 10318–10325.
53. Kovacevic, D.; van der Burgh, S.; de Keizer, A.; Stuart, M.A.C. Kinetics of formation and dissolution of weak polyelectrolyte multilayers: Role of salt and free polyions. *Langmuir* **2002**, *18*, 5607–5612.
54. Tedeschi, C.; Mohwald, H.; Kirstein, S. Polarity of layer-by-layer deposited polyelectrolyte films as determined by pyrene fluorescence. *J. Am. Chem. Soc.* **2001**, *123*, 954–960.
55. Schneider, A.; Vodouhê, C.; Richert, L.; Francius, G.; le Guen, E.; Schaaf, P.; Voegel, J.-C.; Frisch, B.; Picart, C. Multifunctional polyelectrolyte multilayer films: Combining mechanical resistance, biodegradability, and bioactivity. *Biomacromolecules* **2007**, *8*, 139–145.
56. Wang, X.F.; Ji, J. Postdiffusion of oligo-peptide within exponential growth multilayer films for localized peptide delivery. *Langmuir* **2009**, *25*, 11664–11671.
57. Riva, E.R.; Desii, A.; Sartini, S.; la Motta, C.; Mazzolai, B.; Mattoli, V. PMMA/polysaccharides nanofilm loaded with adenosine deaminase inhibitor for targeted anti-inflammatory drug delivery. *Langmuir* **2013**, *29*, 13190–13197.
58. Chuang, H.F.; Smith, R.C.; Hammond, P.T. Polyelectrolyte multilayers for tunable release of antibiotics. *Biomacromolecules* **2008**, *9*, 1660–1668.

59. Ball, V. Organic and inorganic dyes in polyelectrolyte multilayer films. *Materials* **2012**, *5*, 2681–2704.
60. Pavlukhina, S.; Sukhishvili, S. Polymer assemblies for controlled delivery of bioactive molecules from surfaces. *Adv. Drug Deliv. Rev.* **2011**, *63*, 822–836.
61. Lasic, D.D. *Liposomes: From Physics to Applications*; Elsevier: Amsterdam, The Netherlands, 1993.
62. Lasic, D.D.; Papahadjopoulos, D. *Medical Applications of Liposomes*; Elsevier: Amsterdam, The Netherlands, 1998.
63. Graff, A.; Winterhalter, M.; Meier, W. Nanoreactors from polymer-stabilized liposomes. *Langmuir* **2001**, *17*, 919–923.
64. Barenholz, Y. Liposome application: problems and prospects. *Curr. Opin. Colloid Interface Sci.* **2001**, *6*, 66–77.
65. Christensen, S.M.; Stamou, D. Surface-based lipid vesicle reactor systems: Fabrication and applications. *Soft Matter* **2007**, *3*, 828–836.
66. Yoshina-Ishii, C.; Miller, G.P.; Kraft, M.L.; Kool, E.T.; Boxer, S.G. General method for modification of liposomes for encoded assembly on supported bilayers. *J. Am. Chem. Soc.* **2005**, *127*, 1356–1357.
67. Chifen, A.N.; Forch, R.; Knoll, W.; Cameron, P.J.; Khor, H.L.; Williams, T.L.; Jenkins, A.T.A. Attachment and phospholipase A2-induced lysis of phospholipid bilayer vesicles to plasmopolymerized maleic anhydride/SiO₂ multilayers. *Langmuir* **2007**, *23*, 6294–6298.
68. Richter, R.P.; Berat, R.; Brisson, A.R. Formation of solid-supported lipid bilayers: An integrated view. *Langmuir* **2006**, *22*, 3497–3505.
69. Reviakine, I.; Brisson, A. Formation of supported phospholipid bilayers from unilamellar vesicles investigated by atomic force microscopy. *Langmuir* **2000**, *16*, 1806–1815.
70. Volodkin, D.; Ball, V.; Schaaf, P.; Voegel, J.-C.; Mohwald, H. Complexation of phosphocholine liposomes with polylysine: Stabilization by surface coverage vs. aggregation. *Biochim. Biophys. Acta* **2007**, *1768*, 280–290.
71. Volodkin, D.; Mohwald, H.; Voegel, J.-C.; Ball, V. Stabilization of negatively charged liposomes by polylysine surface coating: Drug release study. *J. Control. Release* **2007**, *117*, 111–120.
72. Volodkin, D.V.; Ball, V.; Voegel, J.-C.; Möhwald, H.; Dimova, R.; Marchi-Artzner, V. Control of the interaction between membranes and vesicles: Adhesion, fusion and release of dyes. *Colloids Surf. A* **2007**, *303*, 89–96.
73. Volodkin, D.; Schaaf, P.; Mohwald, H.; Voegel, J.-C.; Ball, V. Effective embedding of liposomes into polyelectrolyte multilayered films: The relative importance of lipid-polyelectrolyte and interpolyelectrolyte interactions. *Soft Matter* **2009**, *5*, 1394–1405.
74. Volodkin, D.V.; Arntz, Y.; Schaaf, P.; Mohwald, H.; Voegel, J.-C.; Ball, V. Composite multilayered biocompatible polyelectrolyte films with intact liposomes: Stability and triggered dye release. *Soft Matter* **2008**, *4*, 122–130.
75. Michel, M.; Izquierdo, A.; Decher, G.; Voegel, J.-C.; Schaaf, P.; Ball, V. Layer-by-layer self-assembled polyelectrolyte multilayers with embedded phospholipid vesicles obtained by spraying: Integrity of the vesicles. *Langmuir* **2005**, *21*, 7854–7859.
76. Michel, M.; Vautier, D.; Voegel, J.-C.; Schaaf, P.; Ball, V. Layer-by-layer self-assembled polyelectrolyte multilayers with embedded phospholipid vesicles. *Langmuir* **2004**, *20*, 4835–4839.

77. Volodkin, D.V.; Michel, M.; Schaaf, P.; Voegel, J.-C.; Mohwald, H.; Ball, V. Liposome embedding into polyelectrolyte multilayers: A new way to create drug reservoirs at solid-liquid interfaces. In *Advances in Planar Lipid Bilayers and Liposomes*; Liu, A.L., Ed.; Elsevier: Amsterdam, The Netherlands, 2008; Volume 8.
78. Delcea, M.; Madaboosi, N.; Yashchenok, A.M.; Subedi, P.; Volodkin, D.V.; de Geest, B.G.; Mohwald, H.; Skirtach, A.G. Anisotropic multicompartiment micro- and nano-capsules produced via embedding into biocompatible PLL/HA films. *Chem. Commun.* **2011**, *47*, 2098–2100.
79. Kohler, D.; Madaboosi, N.; Delcea, M.; Schmidt, S.; de Geest, B.G.; Volodkin, D.V.; Möhwald, H.; Skirtach, A.G. Patchiness of embedded particles and film stiffness control through concentration of gold nanoparticles. *Adv. Mater.* **2012**, *24*, 1095–1100.
80. Graf, N.; Albertini, F.; Petit, T.; Reimhult, E.; Voros, J.; Zambelli, T. Electrochemically stimulated release from liposomes embedded in a polyelectrolyte multilayer. *Adv. Funct. Mater.* **2011**, *21*, 1666–1672.
81. Schwinte, P.; Voegel, J.-C.; Picart, C.; Haikel, Y.; Schaaf, P.; Szalontai, B. Stabilizing effects of various polyelectrolyte multilayer films on the structure of adsorbed/embedded fibrinogen molecules: An ATR-FTIR study. *J. Phys. Chem. B* **2001**, *15*, 11906–11916.
82. Haynie, D.T.; Balkundi, S.; Palath, N.; Chakravarthula, K.; Dave, K. Polypeptide multilayer films: role of molecular structure and charge. *Langmuir* **2004**, *20*, 4540–4547.
83. Boulmedais, F.; Schwinte, P.; Gergely, C.; Voegel, J.-C.; Schaaf, P. Secondary structure of polypeptide multilayer films: An example of locally ordered polyelectrolyte multilayers. *Langmuir* **2002**, *18*, 4523–4525.
84. Boulmedais, F.; Ball, V.; Schwinte, P.; Frisch, B.; Schaaf, P.; Voegel, J.-C. Buildup of exponentially growing multilayer polypeptide films with internal secondary structure. *Langmuir* **2003**, *19*, 440–445.
85. Müller, M. Orientation of α -helical poly(L-lysine) in consecutively adsorbed polyelectrolyte multilayers on texturized silicon substrates. *Biomacromolecules* **2001**, *2*, 262–269.
86. Uhlig, K.; Madaboosi, N.; Schmidt, S.; Jager, M.S.; Rose, J.; Duschl, C.; Volodkin, D.V. 3D localization and diffusion of proteins in polyelectrolyte multilayers. *Soft Matter* **2012**, *8*, 11786–11789.
87. Volodkin, D.V.; Balabushevitch, N.G.; Sukhorukov, G.B.; Larionova, N.I. Model system for controlled protein release: pH-sensitive polyelectrolyte microparticles. *STP Pharm. Sci.* **2003**, *13*, 163–170.
88. Volodkin, D.V.; Balabushevitch, N.G.; Sukhorukov, G.B.; Larionova, N.I. Inclusion of proteins into polyelectrolyte microparticles by alternative adsorption of polyelectrolytes on protein aggregates. *Biochemistry (Moscow)* **2003**, *68*, 236–241.
89. Balabushevich, N.G.; Pechenkin, M.A.; Shibanova, E.D.; Volodkin, D.V.; Mikhalechik, E.V. Multifunctional polyelectrolyte microparticles for oral insulin delivery. *Macromol. Biosci.* **2013**, *13*, 1379–1388.
90. Krafft, C.; Dietzek, B.; Popp, J. Raman and CARS microspectroscopy of cells and tissues. *Analyst* **2009**, *134*, 1046–1057.
91. Krafft, C.; Dietzek, B.; Schmitt, M.; Popp, J. Raman and coherent anti-Stokes Raman scattering microspectroscopy for biomedical applications. *J. Biomed. Opt.* **2012**, *17*, 040801.

92. Wang, M.; Benford, M.; Jing, N.; Cote, G.; Kameoka, J. Optofluidic device for ultra-sensitive detection of proteins using surface-enhanced Raman spectroscopy. *Microfluidics Nanofluidics* **2009**, *6*, 411–417.
93. Han, W.P.; Chuang, K.H.; Chang, Y.T.; Olivo, M.; Velan, S.S.; Bhakoo, K.; Townsend, D.; Radda, G.K. Imaging metabolic syndrome. *EMBO Mol. Med.* **2010**, *2*, 196–210.
94. Stetciura, I.Y.; Markin, A.V.; Ponomarev, A.N.; Yakimansky, A.V.; Demina, T.S.; Grandfils, C.; Volodkin, D.V.; Gorin, D.A. New surface-enhanced Raman scattering platforms: Composite calcium carbonate microspheres coated with astralen and silver nanoparticles. *Langmuir* **2013**, *29*, 4140–4147.
95. Crouzier, T.; Picart, C. Ion pairing and hydration in polyelectrolyte multilayer films containing polysaccharides. *Biomacromolecules* **2009**, *10*, 433–442.
96. Srivastava, S.; Ball, V.; Podsiadlo, P.; Lee, J.; Ho, P.; Kotov, N.A. Reversible loading and unloading of nanoparticles in “exponentially” growing polyelectrolyte LBL films. *J. Am. Chem. Soc.* **2008**, *130*, 3748–3749.
97. Skirtach, A.G.; Volodkin, D.V.; Mohwald, H. Bio-interfaces-interaction of PLL/HA thick films with nanoparticles and microcapsules. *ChemPhysChem* **2010**, *11*, 822–829.
98. Whitesides, G.M.; Ostuni, E.; Takayama, S.; Jiang, X.Y.; Ingber, D.E. Soft lithography in biology and biochemistry. *Annu. Rev. Biomed. Eng.* **2001**, *3*, 335–373.
99. Fukuda, J.; Khademhosseini, A.; Yeh, J.; Eng, G.; Cheng, J.J.; Farokhzad, O.C.; Langer, R. Micropatterned cell co-cultures using layer-by-layer deposition of extracellular matrix components. *Biomaterials* **2006**, *27*, 1479–1486.
100. Khademhosseini, A.; Suh, K.Y.; Yang, J.M.; Eng, G.; Yeh, J.; Levenberg, S.; Langer, R. Layer-by-layer deposition of hyaluronic acid and poly-L-lysine for patterned cell co-cultures. *Biomaterials* **2004**, *25*, 3583–3592.
101. Richert, L.; Boulmedais, F.; Lavallo, P.; Mutterer, J.; Ferreux, E.; Decher, G.; Schaaf, P.; Voegel, J.C.; Picart, C. Improvement of stability and cell adhesion properties of polyelectrolyte multilayer films by chemical cross-linking. *Biomacromolecules* **2004**, *5*, 284–294.
102. Ricotti, L.; Taccola, S.; Bernardeschi, I.; Pensabene, V.; Dario, P.; Menciassi, A. Quantification of growth and differentiation of C2C12 skeletal muscle cells on PSS–PAH-based polyelectrolyte layer-by-layer nanofilms. *Biomed. Mater.* **2011**, *6*, 031001.
103. Ren, K.F.; Crouzier, T.; Roy, C.; Picart, C. Polyelectrolyte multilayer films of controlled stiffness modulate myoblast cell differentiation. *Adv. Funct. Mater.* **2008**, *18*, 1378–1389.
104. Madaboosi, N.; Uhlig, K.; Jäger, M.S.; Möhwald, H.; Duschl, C.; Volodkin, D.V. Microfluidics as a tool to understand the build-up mechanism of exponential-like growing films. *Macromol. Rapid Commun.* **2012**, *33*, 1775–1779.
105. Chien, H.W.; Chang, T.Y.; Tsai, W.B. Spatial control of cellular adhesion using photo-crosslinked micropatterned polyelectrolyte multilayer films. *Biomaterials* **2009**, *30*, 2209–2218.
106. Timko, B.P.; Dvir, T.; Kohane, D.S. Remotely triggerable drug delivery systems. *Adv. Mater.* **2010**, *22*, 4925–4943.
107. Malcher, M.; Volodkin, D.; Heurtault, B.; Andre, P.; Schaaf, P.; Mohwald, H.; Voegel, J.-C.; Sokolowski, A.; Ball, V.; Boulmedais, F.; *et al.* Embedded silver ions-containing liposomes in polyelectrolyte multilayers: Cargos films for antibacterial agents. *Langmuir* **2008**, *24*, 10209–10215.

108. Volodkin, D.V.; Skirtach, A.G.; Mohwald, H. Near-IR remote release from assemblies of liposomes and nanoparticles. *Angew. Chem. Int. Ed.* **2009**, *48*, 1807–1809.
109. Volodkin, D.; Skirtach, A.; Madaboosi, N.; Blacklock, J.; von Klitzing, R.; Lankenau, A.; Duschl, C.; Mohwald, H. IR-light triggered drug delivery from micron-sized polymer biocoatings. *J. Controll. Release* **2010**, *148*, e70–e71.
110. Harris, J.J.; DeRose, P.M.; Bruening, M.L. Synthesis of passivating, nylon-like coatings through cross-linking of ultrathin polyelectrolyte films. *J. Am. Chem. Soc.* **1999**, *121*, 1978–1979.
111. Lee, S.W.; Kim, B.-S.; Chen, S.; Shao-Horn, Y.; Hammond, P.T. Layer-by-layer assembly of all carbon nanotube ultrathin films for electrochemical applications. *J. Am. Chem. Soc.* **2009**, *131*, 671–679.
112. Skirtach, A.G.; Dejognat, C.; Braun, D.; Susha, A.S.; Rogach, A.L.; Sukhorukov, G.B. Nanoparticles distribution control by polymers: Aggregates vs. nonaggregates. *J. Phys. Chem. C* **2007**, *111*, 555–564.
113. Volodkin, D.; Skirtach, A.; Möhwald, H. Bioapplications of light-sensitive polymer films and capsules assembled using the layer-by-layer technique. *Polym. Int.* **2012**, *61*, 673–679.
114. Volodkin, D.V.; Delcea, M.; Mohwald, H.; Skirtach, A.G. Remote near-IR light activation of a hyaluronic acid/poly(L-lysine) multilayered film and film-entrapped microcapsules. *ACS Appl. Mater. Interfaces* **2009**, *1*, 1705–1710.
115. Pechenkin, M.A.; Mohwald, H.; Volodkin, D.V. pH- and salt-mediated response of layer-by-layer assembled PSS/PAH microcapsules: Fusion and polymer exchange. *Soft Matter* **2012**, *8*, 8659–8665.
116. Carregal-Romero, S.; Ochs, M.; Rivera-Gil, P.; Ganas, C.; Pavlov, A.M.; Sukhorukov, G.B.; Parak, W.J. NIR-light triggered delivery of macromolecules into the cytosol. *J. Controll. Release* **2012**, *159*, 120–127.
117. Javier, A.M.; del Pino, P.; Bedard, M.F.; Ho, D.; Skirtach, A.G.; Sukhorukov, G.B.; Plank, C.; Parak, W.J. Photoactivated release of cargo from the cavity of polyelectrolyte capsules to the cytosol of cells. *Langmuir* **2008**, *24*, 12517–12520.
118. Skirtach, A.G.; Dejognat, C.; Braun, D.; Susha, A.S.; Rogach, A.L.; Parak, W.J.; Möhwald, H.; Sukhorukov, G.B. The role of metal nanoparticles in remote release of encapsulated materials. *Nano Lett.* **2005**, *5*, 1371–1377.
119. Skirtach, A.G.; Karageorgiev, P.; Bedard, M.F.; Sukhorukov, G.B.; Mohwald, H. Reversibly permeable nanomembranes of polymeric microcapsules. *J. Am. Chem. Soc.* **2008**, *130*, 11572–11573.
120. Volodkin, D.V.; Schmidt, S.; Fernandes, P.; Larionova, N.I.; Sukhorukov, G.B.; Duschl, C.; Möhwald, H.; von Klitzing, R. One-step formulation of protein microparticles with tailored properties: Hard templating at soft conditions. *Adv. Funct. Mater.* **2012**, *22*, 1914–1922.
121. Schmidt, S.; Behra, M.; Uhlig, K.; Madaboosi, N.; Hartmann, L.; Duschl, C.; Volodkin, D. Mesoporous protein particles through colloidal CaCO₃ templates. *Adv. Funct. Mater.* **2013**, *23*, 116–123.
122. Schmidt, S.; Volodkin, D. Microparticulate biomolecules by mild CaCO₃ templating. *J. Mater. Chem. B* **2013**, *1*, 1210–1218.

123. Schmidt, S.; Uhlig, K.; Duschl, C.; Volodkin, D. Stability and cell uptake of calcium carbonate templated insulin microparticles. *Acta Biomater.* **2014**, *10*, 1423–1430.
124. Volodkin, D. CaCO₃ templated micro-beads and -capsules for bioapplications. *Adv. Colloid Interface Sci.* **2014**, *207*, 306–324.
125. Volodkin, D.V.; von Klitzing, R.; Möhwald, H. Pure protein microspheres by calcium carbonate templating. *Angew. Chem. Int. Ed.* **2010**, *49*, 9258–9261.
126. Behra, M.; Azzouz, N.; Schmidt, S.; Volodkin, D.V.; Mosca, S.; Chanana, M.; Seeberger, P.H.; Hartmann, L. Magnetic porous sugar-functionalized PEG microgels for efficient isolation and removal of bacteria from solution. *Biomacromolecules* **2013**, *14*, 1927–1935.
127. Behra, M.; Schmidt, S.; Hartmann, J.; Volodkin, D.V.; Hartmann, L. Synthesis of porous PEG microgels using CaCO₃ microspheres as hard templates. *Macromol. Rapid Commun.* **2012**, *33*, 1049–1054.
128. Sergeeva, A.; Gorin, D.; Volodkin, D. Polyelectrolyte microcapsule arrays: Preparation and biomedical applications. *BioNanoScience* **2013**, *4*, 1–14.
129. Volodkin, D. Colloids of pure proteins by hard templating. *Colloid Polym. Sci.* **2014**, in press.

© 2014 by the authors; licensee MDPI, Basel, Switzerland. This article is an open access article distributed under the terms and conditions of the Creative Commons Attribution license (<http://creativecommons.org/licenses/by/3.0/>).